

# The first electrochemical sensor for determination of mangiferin based on an ionic liquid–graphene nanosheets paste electrode

Somayeh Tajik · Mohammad Ali Taher · Hadi Beitollahi

Received: 1 November 2013 / Revised: 21 December 2013 / Accepted: 26 December 2013 / Published online: 11 January 2014  
© Springer-Verlag Berlin Heidelberg 2014

**Abstract** A novel carbon paste electrode modified with graphene nanosheets and an ionic liquid (*n*-hexyl-3-methylimidazolium hexafluoro phosphate) was fabricated and used for the electrochemical study of mangiferin for the first time. This modified electrode offers a considerable improvement in voltammetric sensitivity toward mangiferin, compared to the bare electrode. Square wave voltammetry (SWV) exhibits a linear dynamic range from  $5.0 \times 10^{-8}$  to  $2.0 \times 10^{-4}$  M and a detection limit of 20.0 nM for mangiferin. Finally, the proposed method was successfully applied to the determination of mangiferin in real samples such as serum and urine.

**Keywords** Mangiferin · Graphene nanosheets · Modified electrode · Voltammetry

## Introduction

Graphene is an one-atom-thick planar sheet of  $sp^2$ -bonded carbon atoms that is densely packed in a honey-comb crystal lattice. It is the latest nano scale form of carbon to be discovered and is the current hottest topic in material science. Due to

its unique electronic properties, rich edge defects, large surface area, and strong mechanical strength [1]; it exhibits remarkable electrocatalytic and sensing properties [2–7].

Ionic liquids (ILs) have been generating increasing interest over the last decade [8–10]. ILs have a great potential for possible electrochemical applications because these compounds possess high thermal stability, no volatility, high polarity, large viscosity, high intrinsic conductivity, and wide electrochemical windows [11–13].

Mangiferin (Scheme 1) was originally isolated from *Mangifera indica* L. (Anacardiaceae) [14] and can be found in at least 16 plant families including Anacardiaceae, Iridaceae, and Gentianaceae [15]. As the active flavonoid compound of many eutherapeutic traditional Chinese herbs, mangiferin is receiving considerable attention in medical and nutritional research. Mangiferin is reported to have various pharmacological effects, including antioxidation [16], antitumor activity [17], anti-HIV activity [17], immunomodulation [18], anti-inflammation [19], antidiabetic activity [20], and hepatoprotective activity [21].

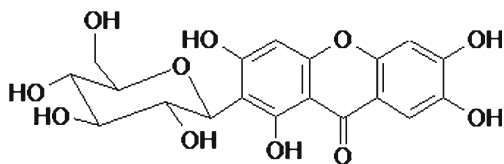
HPLC alone or HPLC combined with mass spectrometry [22] is widely employed for determination of mangiferin quality and quantity in pharmaceutical, pharmacokinetic, or pharmacological studies. Although HPLC is a reliable method and LC–MS has very powerful resolution for the detection of mangiferin and other flavonoid compounds, they remain a costly procedure. Compare to HPLC methods, electrochemical methods may be more applicable because they are less expensive, more convenient, more selective, and sensitive. There is no need for derivatization or time-consuming extraction steps in comparison with other techniques because of less sensitivity of electroanalytical methods to the matrix effects.

Electrochemical techniques in the field of pharmaceutical analysis have developed due to their simplicity, reasonable accuracy and precision, low cost, and rapidity [23–33].

S. Tajik (✉) · M. A. Taher  
Department of Chemistry, Shahid Bahonar University of Kerman,  
P.O. Box 76175-133, Kerman, Iran  
e-mail: tajik\_s1365@yahoo.com

S. Tajik  
Young Researchers Society, Shahid Bahonar University of Kerman,  
P.O. Box 76175-133, Kerman, Iran

H. Beitollahi  
Environment Department, Institute of Science and High Technology  
and Environmental Sciences, Graduate University of Advanced  
Technology, Kerman, Iran



**Scheme 1** Structure of mangiferin

Carbon-paste electrodes (CPEs) are widely utilized to perform the electrochemical determinations of a variety of biological and pharmaceutical species owing to their low residual current and noise, ease of fabrication, wide anodic and cathodic potential ranges, rapid surface renewal, and low cost. Moreover, chemically modified electrodes (CMEs) can be easily prepared by adding different substances to the bulk of CPEs in order to increase sensitivity, selectivity, and rapidity of determinations [34–44].

In the present work, we describe the preparation of a new carbon paste electrode modified with an ionic liquid and graphene nanosheets (IL-G-CPE) and investigate its performance for the determination of mangiferin in aqueous solutions for the first time.

## Experimental

### Apparatus and chemicals

The electrochemical measurements were performed with an Autolab potentiostat/galvanostat (PGSTAT 302N, Eco Chemie, the Netherlands). The experimental conditions were controlled with General Purpose Electrochemical System (GPES) software. A conventional three electrode cell was used at  $25 \pm 1$  °C. An Ag/AgCl/KCl (3.0 M) electrode, a platinum wire, and IL-G-CPE were used as the reference, auxiliary, and working electrodes, respectively. A Metrohm 710 pH meter was used for pH measurements.

Mangiferin was purchased from Sigma Aldrich Company (USA), and all of the other reagents were of analytical grade and were obtained from Merck (Darmstadt, Germany). The buffer solutions were prepared from orthophosphoric acid and its salts in the pH range of 2.0–11.0.

### Synthesis of graphene nanosheets

Graphene nanosheets were synthesized from natural graphite flakes based on the modified Hummers and Offeman's method [45, 46]. In a typical synthesis process, 1.0 g of pristine graphite flakes was immersed in 50 mL of formic acid, and then sonicated for 2 h at room temperature. These resulting graphite plates were washed with acetone, and then dried in an oven at 95 °C for 12 h. Then, 100 mL  $\text{H}_2\text{SO}_4$  (95 %) was added into a 500-mL flask, and cooled by immersion in an ice

bath followed by stirring. About 1.0 g treated graphite powder and 0.5 g  $\text{NaNO}_3$  were added under vigorous stirring to avoid agglomeration. After the graphite powder was well dispersed, 3 g  $\text{KMnO}_4$  was added gradually under stirring and cooling so that the temperature of the mixture was maintained below 10 °C. The mixture was stirred for 2 h and diluted with deionised double-distilled water (in an ice bath). After that, 25 ml 15 %  $\text{H}_2\text{O}_2$  was slowly added to the mixture until the color of the mixture changed to brilliant yellow, indicating fully oxidized graphite. The as-obtained graphite oxide slurry was re-dispersed in deionised double-distilled water and then exfoliated to generate graphene oxide nanosheets by sonication for 2 h. Then, the solution was filtered and washed with diluted HCl solution to remove metal ions. Finally, the product was washed with deionised double-distilled water until the solution became acid free, and dried under vacuum at 50 °C. A typical TEM for synthesized graphene nanosheets is shown in Fig. 1.

### Preparation of the electrode

IL-G-CPEs were prepared by mixing 0.2 g of graphene with 0.8 g graphite powder and approximately, ~0.8 mL of ionic liquids with a mortar and pestle. The paste was then packed into the end of a glass tube (ca. 3.4 mm i.d. and 15 cm long). A copper wire inserted into the carbon paste provided the electrical contact.

For comparison, ionic liquid/carbon paste electrode in the absence of graphene (IL-CPE) consistent of ionic liquid and graphite powder, graphene carbon paste electrode (G-CPE) consistent of graphene, graphite powder and paraffin oil, and bare carbon paste electrode (CPE) consistent of graphite powder and paraffin oil were also prepared in the same way.

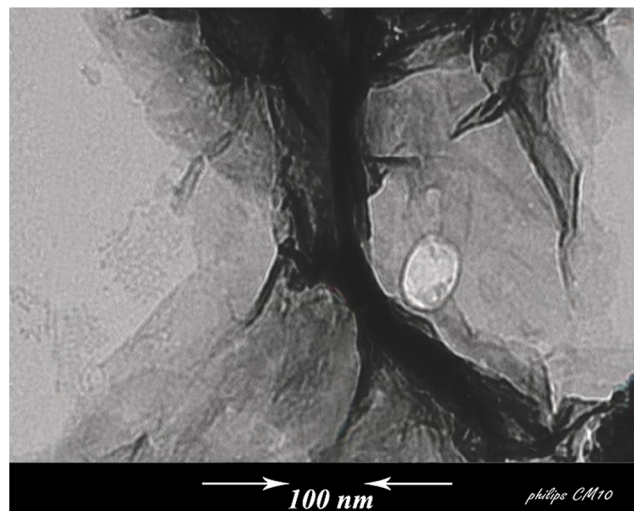


**Fig. 1** TEM image of synthesized graphen nanosheets

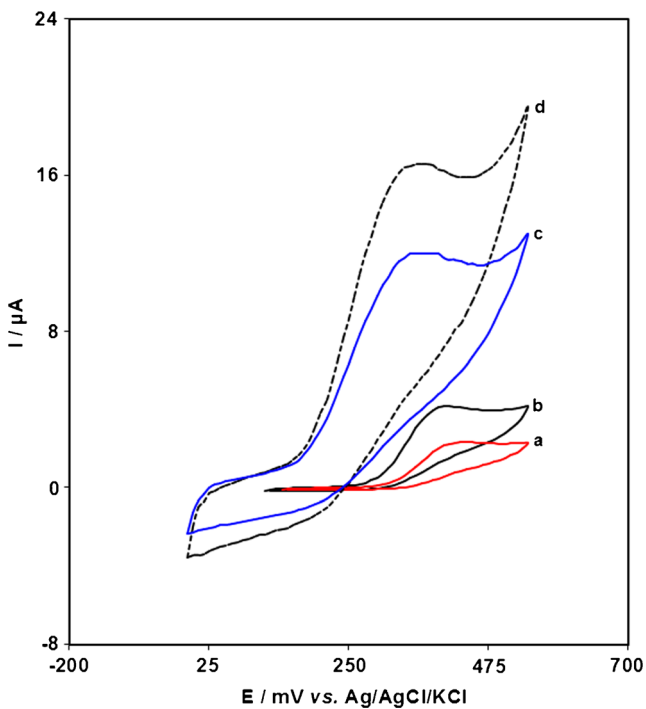
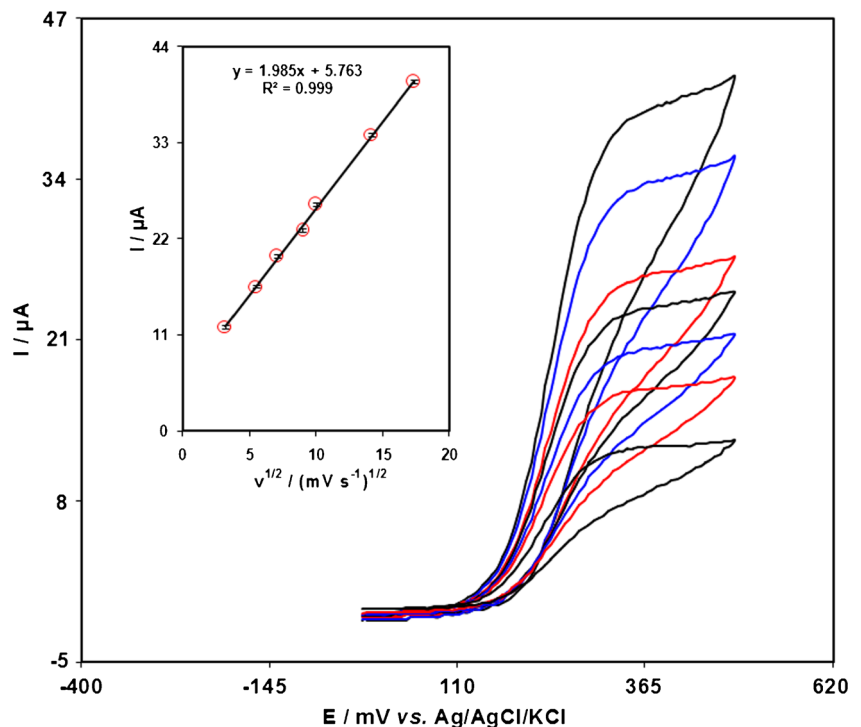


**Fig. 2** Cyclic voltammograms of *a* CPE, *b* G-CPE, *c* IL-CPE, and *d* IL-G-CPE in the presence of 100.0 μM mangiferin at a pH 6.0, respectively. In all cases the scan rate was 30 mV s<sup>-1</sup>

Procedure of real samples preparation

The serum sample was centrifuged and then after filtering, diluted with PBS (pH 6.0) without any further treatment. The diluted serum sample was spiked with different amounts of mangiferin.

**Fig. 3** CVs of IL-G-CPE in 0.1 M PBS (pH 6.0) containing 100.0 μM mangiferin at various scan rates; from inner to outer correspond to 10, 30, 50, 80, 100, 200, and 300 mV s<sup>-1</sup>, respectively. *Inset* variation of anodic peak current vs. square root of scan rate



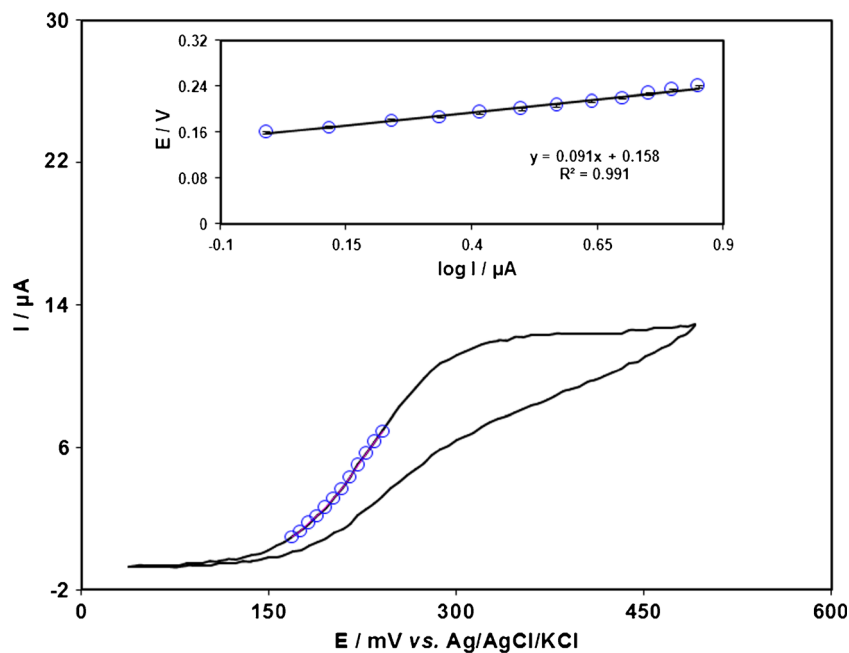
Urine samples were stored in a refrigerator immediately after collection. Ten milliliters of the sample was centrifuged for 15 min at 2,000 rpm. The supernatant was filtered out using a 0.45-μm filter. Then, different volumes of the solution were transferred into a 10-mL volumetric flask and were diluted to the mark with PBS (pH 6.0). The diluted urine sample was spiked with different amounts of mangiferin.

Result and discussion

Electrochemical behavior of mangiferin at the surface of various electrodes

Figure 2 displays cyclic voltammetric responses from the electrochemical oxidation of 100.0 μM mangiferin at the surface of IL-G-CPE (curve d), IL-CPE (curve c), G-CPE (curve b), and bare CPE (curve a). The results showed that the oxidation of mangiferin is very weak at the surface of the bare CPE, but in the presence of ILs in CPE could enhance the peak current and decrease the oxidation potential (decreasing the overpotential). A substantial negative shift of the currents starting from oxidation potential for mangiferin and dramatic increase of the current indicates the catalytic ability of IL-G-CPE (curve d) and IL-CPE (curve c) to mangiferin oxidation. The results showed that the combination of G and the ionic liquid (curve d) definitely improved the characteristics of mangiferin oxidation. However, IL-G-CPE shows much higher anodic peak current for the oxidation of mangiferin

**Fig. 4** Cyclic voltammogram (at  $10 \text{ mV s}^{-1}$ ) of an IL-G-CPE in 0.1 M PBS (pH 6.0) containing  $100.0 \mu\text{M}$  mangiferin. The *points* are the data used in the Tafel plot. The *inset* shows the Tafel plot derived from the cyclic voltammogram



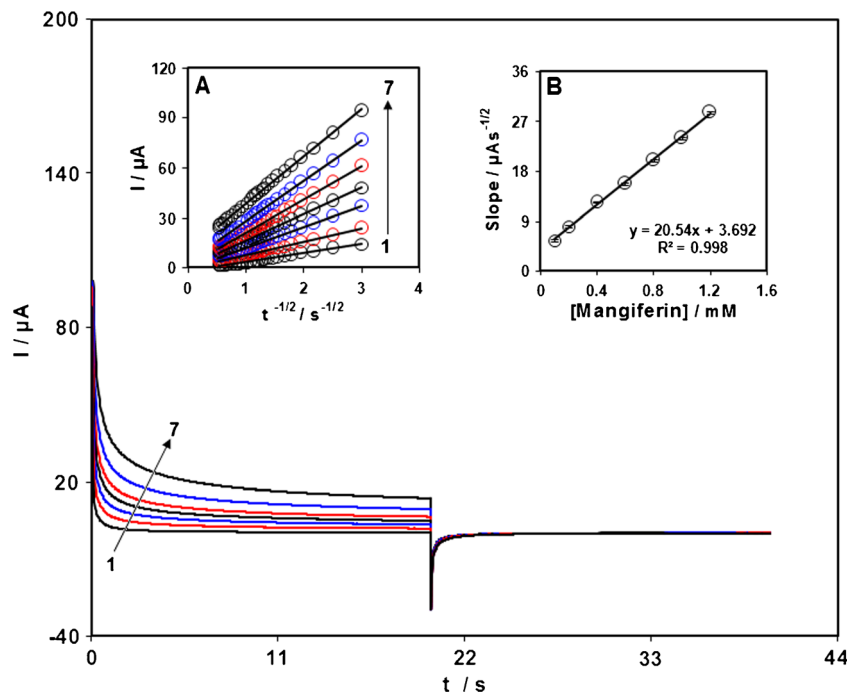
compared to IL-CPE, indicating that the combination of G and IL has significantly improved the performance of the electrode toward mangiferin oxidation.

#### Effect of variables

The electrochemical behavior of mangiferin ( $\text{p}K_{\text{a}1}=6.52$ ,  $\text{p}K_{\text{a}2}=7.97$ ,  $\text{p}K_{\text{a}3}=9.44$ ,  $\text{p}K_{\text{a}4}=12.10$  [47]), is dependent on the pH value of the aqueous solution, therefore, pH optimization of the solution seems to be necessary. The effect of

solution pH on electrochemical responses of mangiferin at the surface of IL-G-CPE was investigated over a pH range of 2.0 to 10.0 using cyclic voltammetry. The results showed that the peak current reached to a maximum value at pH 6.0. The results also showed a linear negative shift for the variation of the anodic peak potential of mangiferin with increasing the solution pH (from 2.0 to 10.0) with a slope of  $-49 \text{ mV/pH}$  unit, which indicates that the total numbers of electrons and protons taking part in the charge transfer were the same for mangiferin.

**Fig. 5** Chronoamperograms obtained at IL-G-CPE in 0.1 M PBS (pH 6.0) for different concentration of mangiferin. The numbers 1–7 correspond to 0.1, 0.2, 0.4, 0.6, 0.8, 1.0, and 1.2 mM of mangiferin. *Inset A* plots of  $I$  vs.  $t^{-1/2}$  obtained from chronoamperograms 1–7. *B* Plot of the slope of the straight lines against mangiferin concentration



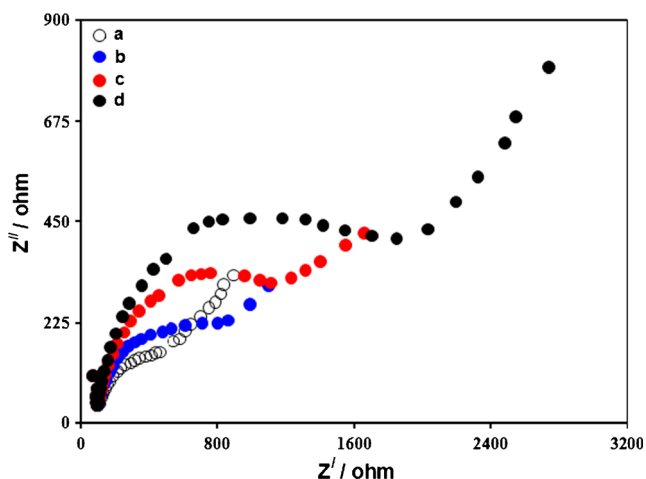


**Fig. 6** Nyquist plots of *a* CPE, *b* G-CPE, *c* IL-CPE, and *d* IL-G-CPE in the presence of 100.0 μM mangiferin at a pH 6.0 PBS, respectively

The effect of potential scan rates on the oxidation current of mangiferin has been studied (Fig. 3). The results showed that increasing in the potential scan rate induced an increase in the peak current. In addition, the oxidation process is diffusion controlled as deduced from the linear dependence of the anodic peak current ( $I_p$ ) on the square root of the potential scan rate ( $\nu^{1/2}$ ) over a wide range from 10 to 300  $\text{mV s}^{-1}$ .

Figure 4 shows the cyclic voltammogram of an IL-G-CPE obtained in 0.1 M PBS (pH 6.0) containing 0.1 mM mangiferin, with a sweep rate of 10  $\text{mV s}^{-1}$ . The points show the rising part of the voltammogram (known as the Tafel region), which is affected by the electron transfer kinetics between mangiferin and IL-G-CPE. If deprotonation of mangiferin is a sufficiently fast step, the number of electrons

**Table 1** Determination of mangiferin in serum and urine samples

Sample	Added	Expected	Found	Recovery (%)	RSD (%)
Serum	5.0	5.0	4.9	98.0	2.5
	15.0	15.0	15.6	104.0	3.3
	25.0	25.0	25.4	101.6	1.7
	35.0	35.0	34.7	99.1	2.4
Urine	10.0	10.0	10.3	103.0	3.4
	20.0	20.0	19.8	99.0	2.1
	30.0	30.0	30.4	101.3	2.9
	40.0	40.0	39.4	98.5	1.8

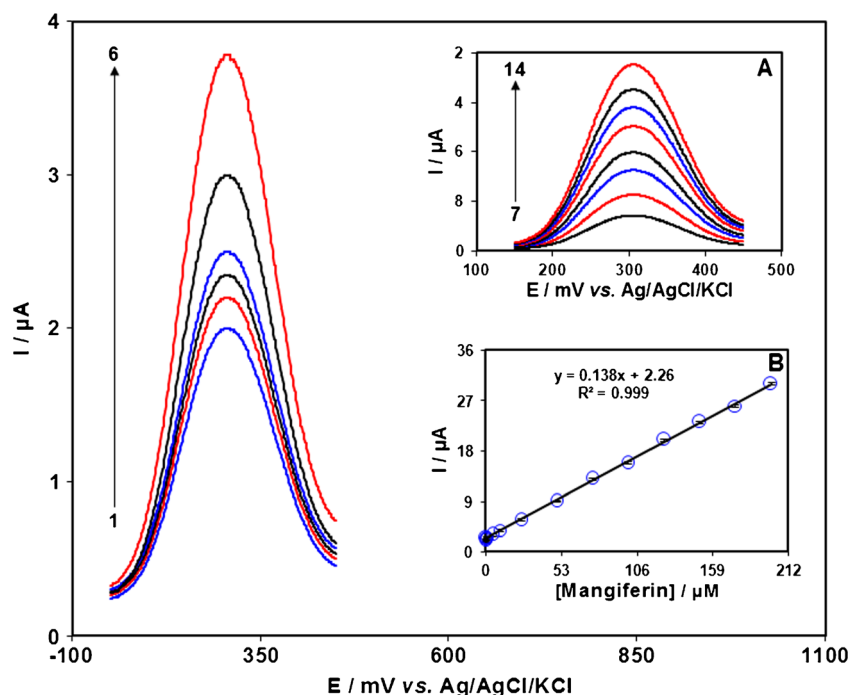
All the concentrations are in micromoles ( $n=5$ )

involved in the rate determining step can be estimated from the slope of the Tafel plot. The inset of Fig. 4 shows a Tafel plot that was drawn from points of the Tafel region of the cyclic voltammogram. The Tafel slope of 0.091 V obtained in this case agrees well with the involvement of one electron in the rate determining step of the electrode process, assuming a charge transfer coefficient of  $\alpha=0.35$ .

Chronoamperometric measurements

Chronoamperometric measurements of mangiferin at IL-G-CPE were carried out by setting the working electrode potential at 0.45 V (at the first potential step) and at 0.0 V (at second potential step) vs. Ag/AgCl/KCl (3.0 M) for the various concentrations of mangiferin in PBS (pH 6.0; Fig. 5). For an electroactive material (mangiferin in this case) with a diffusion coefficient of  $D$ , the current observed for the electrochemical

**Fig. 7** SWVs of IL-G-CPE in 0.1 M PBS (pH 6.0) containing different concentrations of mangiferin. Numbers 1–14 correspond to 0.05, 0.1, 0.5, 1.0, 5.0, 10.0, 25.0, 50.0, 75.0, 100.0, 125.0, 150.0, 175.0, and 200.0 μM of mangiferin. Inset B show the plots of the peak current as a function of mangiferin concentration in the range of 0.05–200.0 μM



reaction at the mass transport limited condition is described by the Cottrell equation [48]. Experimental plots of  $I$  vs.  $t^{-1/2}$  were employed, with the best fits for different concentrations of mangiferin (Fig. 5a). The slopes of the resulting straight lines were then plotted vs. mangiferin concentration (Fig. 5b). From the resulting slope and Cottrell equation the mean value of the  $D$  was found to be  $4.38 \times 10^{-6}$  cm<sup>2</sup>/s.

#### Electrochemical impedance spectroscopy

Electrochemical impedance spectroscopy was also employed to study the oxidation of mangiferin at the surface of various electrodes. Figure 6 shows Nyquist diagrams of IL-G-CPE (curve d), IL-CPE (curve c), G-CPE (curve b), and bare CPE (curve a) in the presence of mangiferin at pH 6.0. Nyquist diagram consists of a semicircle and straight line with a slope of nearly 45° that is due to the occurrence of mass transport process via diffusion. The semicircle diameters of Nyquist plot reflect the electron transfer resistance ( $R_{ct}$ ), which is from the electron transfer of the mangiferin solution. The results showed that for IL-G-CPE (curve d), the diameter of the semicircle is smaller than the other electrodes, which is due to the presence of high conductive IL and G in the carbon paste. All these results indicated that mangiferin can successfully oxidize on the surface of IL-G-CPE.

#### Calibration plot and limit of detection

The peak current of mangiferin oxidation at the surface of the modified electrode can be used for determination of mangiferin in solution. Therefore, square wave voltammetry (SWV) experiments were done for different concentrations of mangiferin (Fig. 7). The oxidation peak currents of mangiferin at the surface of a modified electrode were proportional to the concentration of the mangiferin within the ranges  $5.0 \times 10^{-8}$  to  $2.0 \times 10^{-4}$  M with detection limit ( $3\sigma$ ) of 20.0 nM.

#### The repeatability and stability of IL-G-CPE

The long-term stability of the IL-G-CPE was tested over a 3-week period. When CVs were recorded after the modified electrode was stored in atmosphere at room temperature, the peak potential for mangiferin oxidation was unchanged and the current signals showed less than 2.6 % decrease relative to the initial response. The antifouling properties of the modified electrode toward mangiferin oxidation and its oxidation products were investigated by recording the cyclic voltammograms of the modified electrode before and after use in the presence of mangiferin. Cyclic voltammograms were recorded in the presence of mangiferin after having cycled the potential 20 times at a scan rate of 30 mV s<sup>-1</sup>. The peak

potentials were unchanged and the currents decreased by less than 2.4 %. Therefore, at the surface of IL-G-CPE, not only the sensitivity increase, but the fouling effect of the analyte and its oxidation product also decreases.

#### Real sample analysis

In order to evaluate the analytical applicability of the proposed method, also it was applied to the determination of mangiferin in serum and urine samples. The results are given in Table 1.

#### Conclusion

Electrochemical behavior of mangiferin was studied for the first time at the surface of a graphene nanosheet/ionic liquid carbon paste electrode. The proposed modified electrode presented a low detection limit and good linear range and reproducibility which make it a suitable mangiferin sensor for practical applications.

#### References

- Westervelt RM (2008) *Science* 320:324
- Mallesha M, Manjunatha R, Nethravathi C, Suresh GS, Rajamathi M, Melo JS, Venkatesha TV (2011) *Bioelectrochemistry* 81:104
- Gan T, Sun J, He M, Wang L (2013) *Ionics*. doi:10.1007/s11581-013-0951-9
- Wan Q, Liu Y, Wang Z, Wei W, Li B, Zou J, Yang N (2013) *Electrochem Commun* 29:29
- Sun W, Liu J, Ju X, Zhang L, Qi X, Hui N (2013) *Ionics* 19:657
- Xi F, Zhao D, Wang X, Chen P (2013) *Electrochem Commun* 26:81
- Sun W, Liu J, Wang X, Li T, Li G, Wu J, Zhang L (2012) *Mater Sci Eng* 32:2129
- Afkhami A, Madrakian T, Shirzadmehr A, Bagheri H, Tabatabaee M (2012) *Ionics* 18:881
- Banks CE, Compton RG (2006) *Analyst* 131:15
- Ensafī AA, Rezaei B, Krimi-Maleh H (2011) *Ionics* 17:659
- Sun W, Guo CX, Zhu Z, Li CM (2009) *Electrochem Commun* 11: 2105
- Zhuang RR, Jian FF, Wang KF (2010) *Ionics* 16:661
- Shiddiky MJA, Torriero AAJ (2011) *Biosens Bioelectron* 26:775
- Haynes LJ (1963) *Adv Carbohydr Chem* 18:227
- Sanugul K, Akao T, Li Y, Kakiuchi N, Nakamura N, Hattori M (2005) *Biol Pharm Bull* 28:1672
- Sanchez GM, Re L, Giuliani A, Nunez-Selles AJ, Davison GP, Leon Fernandez OS (2000) *Pharm Res* 42:565
- Guha S, Ghosal S, Chattopadhyay U (1996) *Chemotherapy* 42:443
- Garcia D, Escalante M, Delgado R, Ubeira FM, Leiro J (2003) *Phytother Res* 17:1203
- Lee HZ, Lin WC, Yeh FT, Lin CN, Wu CH (1998) *Eur J Pharm* 353: 303
- Miura T, Iwamoto N, Kato M, Ichiki H, Kubo M, Komatsu Y (2001) *Biol Pharm Bull* 24:091
- Yoshikawa M, Ninomiya K, Shimoda H, Nishida N, Matsuda H (2002) *Biol Pharm Bull* 25:72

22. Liu Y, Xu F, Zeng X, Yang L, Deng Y, Wu Z, Feng Y, Li X (2010) *J Chromatogr B* 878:3345
23. Huang W, Gan T, Luo S, Zhang S (2013) *Ionics* 19:1303–1307
24. Mokhtari A, Karimi-Maleh H, Ensafi AA, Beitollahi H (2012) *Sens Actuators B* 169:96
25. Biniak S, Pakula M, Darlewski W, S'wia\_tkowski A, Kula P (2009) *J Appl Electrochem* 39:593
26. Gopu G, Muralidharan B, Vedhi C, Manisankar P (2012) *Ionics* 18:231
27. Tajik S, Taher MA, Beitollahi H (2013) *Sens Actuators B* 188:923
28. Yari A, Sepahvand R (2011) *Microchim Acta* 174:321
29. Xu G, Tang L, Liu H (2013) *Ionics* 19:309
30. Taleat Z, Mazloum Ardakani M, Naeimi H, Beitollahi H, Nejati M, Zare HR (2008) *Anal Sci* 24:1039
31. Beitollahi H, Mohadesi A, Khalilizadeh Mahani S, Karimi-Maleh H, Akbari A (2012) *Ionics* 18:703
32. Mohammadi S, Beitollahi H, Mohadesi A (2013) *Sens Lett* 11:388
33. Zhou J, Wang F, Zhang K, Song G, Liu J, Ye B (2012) *Microchim Acta* 178:179
34. Beitollahi H, Raoof JB, Hosseinzadeh R (2011) *Electroanalysis* 23:1934
35. Noroozifar M, Khorasani-Motlagh M, Bemanadi Parizi M, Akbari R (2013) *Ionics* 19:1317
36. Beitollahi H, Raoof JB, Hosseinzadeh R (2011) *Anal Sci* 27:991
37. Aydoğdu G, Zeybek DK, Zeybek B, Pekyardımcı Ş (2013) *J Appl Electrochem* 43:523
38. Mazloum-Ardakani M, Beitollahi H, Amini MK, Mir Khalaf F, Abdollahi-Alibeik M (2010) *Sens Actuators B* 151:243
39. Raoof JB, Ojani R, Beitollahi H (2007) *Electroanalysis* 19:1822
40. Beitollahi H, Ghorbani F (2013) *Ionics* 19:1673
41. Raoof JB, Ojani R, Beitollahi H, Hosseinzadeh R (2006) *Electroanalysis* 18:1193
42. Chicharro M, Zapardiel A, Bermejo E, Moreno M, Madrid E (2002) *Anal Bioanal Chem* 373:277
43. Raoof JB, Ojani R, Beitollahi H, Hosseinzadeh R (2006) *Anal Sci* 22:1213
44. Wang Z, Liu G, Zhang, Wang H (2013) *Ionics* 19:1687
45. Hummers WS, Offeman RE (1958) *J Am Chem Soc* 80:1339
46. Kovtyukhova NI, Ollivier P, Martin RB, Mallouk TE, Chizhik SA, Buzaneva EV, Gorchinskiy AD (1999) *Chem Mater* 11:771
47. Gómez-Zaleta B, Ramírez-Silva MT, Gutiérrez A, González-Vergara E, Güizado-Rodríguez M, Rojas-Hernández A (2006) *Spectrochim Acta* 64:1002
48. Bard AJ, Faulkner LR (2001) *Electrochemical methods fundamentals and applications*, 2nd edn. Wiley, New York